FREIGHT MOBILITY RESEARCH INSTITUTE
College of Engineering & Computer Science
Florida Atlantic University

Project ID: FMRI2017-Y6

SEQUENTIAL SYNCHRONIZATION CONTROL SCHEME FOR FREEWAY TRUCK PLATOONING FORMATION

Final Report

by

Lili Du
lilidu@ufl.edu
https://faculty.eng.ufl.edu/lilidu
University of Florida

Scott S. Washburn
swash@ce.ufl.edu
https://swash.essie.ufl.edu
University of Florida

Mukundhan Narasimhan
mnarasimhan@ufl.edu
University of Florida

for

Freight Mobility Research Institute (FMRI)
Florida Atlantic University
777 Glades Rd.
Boca Raton, FL 33431

March, 2024

ACKNOWLEDGEMENTS

This project was funded by the Freight Mobility Research Institute (FMRI), one of the twenty TIER University Transportation Centers that were selected in this nationwide competition, by the Office of the Assistant Secretary for Research and Technology (OST-R), U.S. Department of Transportation (US DOT).

DISCLAIMER

TABLE OF CONTENTS

EXECUTIVE SUMMARY **1**
1.0 INTRODUCTION **3**
1.1 BACKGROUND 3
1.2 LITERATURE REVIEW ON PLATOON FORMATION 3
1.3 PROBLEM STATEMENT 4
1.4 OBJECTIVE 4
2.0 RESEARCH APPROACH **5**
2.1 DYNAMIC MIXED TRAFFIC ENVIRONMENT 5
2.1.1 Neighboring HDVs, CAVs and Platoon Control 5
2.1.2 Macroscopic Traffic Characteristics 6
3.0 REACTIVE CONTROL **9**
3.1 DESCRIPTION OF MOTION AND CONTROL SCHEME 9
3.2 REACTION TO THE TARGET LEADER BY SPRING-MASS-DAMPER 10
3.3 REACTION TO THE TARGET LEADER BY SPRING-MASS-DAMPER 12
3.4 REACTION TO DISTANT TRAFFIC 13
3.5 OUTPUT OF THE REACTIVE CONTROLLER 14
4.0 SEQUENTIAL TRUCK PLATOON FORMATION ALGORITHM **17**
5.0 EXPERIMENTS **19**
5.1 SIGNIFICANCE OF RESPONDING TO MACROSCOPIC TRAFFIC 19
5.2 MACROSCOPIC TRAFFIC FAVORING PLATOON FORMATION 21
6.0 CONCLUSION **23**
7.0 REFERENCES **25**

LIST OF FIGURES

Figure 1: Representation of the traffic stream, various elements of the reactive controller. 5
Figure 2: Fundamental Diagram 7
Figure 3: Spring function. 10
Figure 4: Damper function. 11
Figure 5: Benefits of responding to the macroscopic traffic 20
Figure 6: Speed of *s*-CAV and the CTM cells during platoon formation. 21
Figure 7: Time taken to form a platoon under various traffic conditions. 21
Figure 8: Flow rate around the s-CAV during platoon formation. 22

EXECUTIVE SUMMARY

Truck platooning has been demonstrated as a promising approach to reduce freeway congestion, engine energy consumption, and associated emissions. However, efficient local-level algorithms to form a truck platoon without jeopardizing surrounding traffic flow's safety and efficiency are still lacking. Motivated by this view, this study developed a Sequential Truck Platoon Formation (StPF) algorithm built upon a Reactive Controller following spring-mass-damper (SMD) control. Specifically, the StPF identifies the pair of connected trucks to form/join a platoon while the Reactive Controller manages the movement of the trucks, adapting to a mixed, hybrid, and dynamic traffic environment on the freeway segment, including adjacent connected and autonomous vehicles following cooperative adaptive cruise control, and non-cooperative human-driven vehicles as well as distant aggregated traffic flow described by Cell Transmission Model (CTM). Numerical experiments highlighted the significance of responding to macroscopic traffic and its impact on successful platoon formation and dynamic order identification. The experiments also indicated that platoon formation is favorable up to Level of Service (LOS) C, by Highway Capacity Manual definitions, and high Connected and Automated Vehicle (CAV) penetration traffic conditions, where it improved the overall traffic flow rate. To further show the merits of truck platoon formation in mixed traffic, it is recommended to study the travel time benefits for both the individual connected truck and the overall network in mixed traffic at various traffic conditions. Quantifying this merit is crucial to build support for implementing platoon formation in the field.

Commented [SW1]: Use of first-person pronouns are not recommended for this type of writing, but if you used it extensively throughout the document, then we may need to let it be at this point.

1.0 INTRODUCTION

1.1 BACKGROUND

Purchase and movement of goods, especially aggravated due to the growth in e-commerce during the pandemic (US Census Bureau, 2024a), has been increasing over the past decade (US Census Bureau, 2024b). Consequently, this has increased truck traffic which contributes substantial greenhouse gas emissions (*US EPA*, 2023) and worsens urban traffic congestion (Mobility Division, 2022). Truck platooning, linking two or more trucks in a convoy that moves in a compact pattern at high speed, has been shown to be a promising solution for combating these issues. When travelling in a straight section of a freeway, studies show that the follower trucks gain aerodynamic benefits that can result in improved fuel efficiency (Zabat *et al*., 1995, Patten *et al*., 2012) and reduced emissions (Barth *et al*., 2005). Additionally, with the recent advancement of autonomy and vehicular communication, Connected Autonomous Vehicles (CAVs) have shown to help significantly with this coordinated driving task (Shladover *et al*., 2015, Van Arem *et al*., 2006) in all aspects.

Motivated by these advantages, platooning control (also called stabling) algorithms have been investigated extensively to ensure the efficiency and safety of truck platooning. External factors such as communication time-delays and uncertainties in vehicle dynamics can interfere with platoon control stability. Such uncertainties can be addressed by using a H_∞ controller, which achieves stabilization by modelling the vehicle control problem as an optimization problem (Gao *et al*., 2016). Further studies by Contet *et al*., (2007), Bang *et al*., (2017), and others have conducted theoretical analysis to guarantee individual vehicle control stability. Li & Guo (2020), Li *et al*., (2020), and others have extended the studies to guarantee platoon string stability, where disturbances at the front of the platoon are not amplified when propagating along the vehicle string (Feng *et al*., 2019). Individual vehicle, string, and traffic flow stability can be ensured while accounting for faults in actuators and discrete inputs (Guo *et al*., 2020). In summary, platoon control is extensively studied and is summarized in Li *et al*., (2017). However, these studies assume that a platoon already exists.

1.2 LITERATURE REVIEW ON PLATOON FORMATION

Efficient algorithms to locally form truck platoons are still nascent. Some initial studies are briefed as follows. Liang *et al*., (2015) and Deng *et al*., (2022) researched how to have one CAV catch up to another on the same lane. Zhang *et al*., (2022) advanced this study by considering two CAVs on different lanes. However, none of these studies consider the interference of Human Driven Vehicles (HDVs). Having recognized this issue, Wang *et al*., (2022) proposed lane-management to separate CAVs and HDVs for forming platoons on their corresponding lanes. Qiu & Du, (2023) advanced these previous studies by developing a Model Predictive Control (MPC) that allows one CAV to catch up with another in a different lane while navigating around a mixed surrounding

Commented [SW2]: Not just e-commerce. I think purchase and movement of goods has been rising steadily for many years (except maybe for the supply-chain issues during the pandemic). We can probably find some statistics somewhere, such as National Retail Federation, American Trucking Association, and Bureau of Transportation Statistics.

Commented [SW3R2]: Sounds good, but you could probably put the references at the end with the rest of the references, rather than as footnotes.

Commented [SW4]: Should explain what this means.

Commented [SW5]: What does this mean?

Commented [MN6R5]: Faults in actuators: Example, we ask for 1 m/s2 longitudinal acceleration, but the vehicle was not able to maintain this acceleration.

Discrete inputs (input quantization): Example, the optimal acceleration is 0.1 m/s2, but the vehicle can only accelerate in multiples of 0.25 m/s2.

Commented [SW7]: Do you mean the technology to form a platoon already exists?

Commented [MN8R7]: Under ideal scenarios, yes. An example of a ideal scenarios is a single lane freeway only CAV traffic.

traffic involving HDVs. However, the MPC optimizer relies on a predefined vehicle order in the target platoon, which limits its application to a platoon formation of multiple vehicles since planning real-time target vehicle sequence in a platoon itself is challenging. More recent merging algorithms for forming the initial short platoon are summarized by Li *et al*. (2022).

1.3 PROBLEM STATEMENT

Existing studies have not fully solved the general truck platoon formation involving multiple trucks scattered in mixed traffic consisting of CAVs and HDVs on multiple lanes. Moreover, it is still unclear if platoon formation algorithms can be applied for truck platoons given that manipulating multiple heavy trucks simultaneously could severely disrupt traffic flow. Finally, the traffic conditions under which implementing truck platooning can improve traffic flow operations are not well understood.

1.4 OBJECTIVE

Motivated by this view, this study seeks to develop a novel Sequential truck Platoon Formation (StPF) algorithm to manage the creation and expansion of a truck platoon and a reactive control scheme that efficiently forms a CAV platoon in a mixed traffic environment while factoring in both neighboring adjacent traffic and distant traffic impacts. Specifically, a subject CAV ($\mathcal{s}$-CAV) is a truck that is seeking another downstream connected truck (target truck) to catch up with and form a short platoon or join an existing neighboring truck platoon $\mathbb{P}$. The target truck or the truck platoon could be on a different lane in the multi-lane freeway segment. Additionally, there could be other HDVs or other CAVs (n-CAVs) that do not want to join the platoon on this segment.

Commented [SW9]: Also determining under what traffic conditions it makes sense to implement the truck platooning.

Commented [SW10]: Move this to the end of Chapter 1.

Commented [SW11]: This reads more like an objective. We need to more clearly describe what the existing 'problem' is, or current deficiency/gap in the state of the art.

2.0 RESEARCH APPROACH

2.1 DYNAMIC MIXED TRAFFIC ENVIRONMENT

To explore this platoon formation problem formally, a straight section of the freeway is considered with $\mathbb{L}$ lanes with individual lane denoted by $l \in \mathbb{L}$. The reactive control for the platoon formation will be performed in discrete timesteps $t \in Z+ := 0, 1, 2, \ldots$ with a uniform time interval $\Delta t > 0$. Let the $\mathcal{s}$-CAV be denoted by $\mathcal{s}$. Its corresponding length, position, lane, speed, and acceleration vectors will be $L_s, x_s(t), l_s(t), v_s(t), u_s(t)$. The platoon, if it exists, contains $\mathbb{P}$ vehicles and their lengths, position, lane, and speed will be $L_p, x_p(t), l_p(t), v_v(t), a_p(t), p \in \mathbb{P}$. The set of vehicles in the platoon is denoted by $\Omega_p(t)$. In particular, the target leader for the $\mathcal{s}$-CAV will be indexed by $\mathcal{p}$. The adjacent HDVs belQong in a set $\Omega_h(t)$, the n-CAVs belong in the set $\Omega_n(t)$. As a result, the set of vehicles, at every timestep, is defined by $\Omega(t) = \Omega_s(t) \cup \Omega_p(t) \cup \Omega_n(t) \cup \Omega_h(t)$. We acknowledge that there can be multiple $\mathcal{s}$-CAVs willing to form/join the platoon at any given timestep. This methodology will first focus on developing the reactive controller for one $\mathcal{s}$-CAV. Then a discussion how to manage the platoon formation when there are multiple $\mathcal{s}$-CAVs willing to join the platoon will be presented.

2.1.1 Neighboring HDVs, CAVs and Platoon Control

First of all, this controller must have the $\mathcal{s}$-CAV react to the dynamics of its neighboring HDVs and CAVs to ensure traffic safety. Among existing HDVs' car-following models, this study uses the Modified Pitt model described by (Cohen, 2002), considering its simple formulation (see (1)) fits the Reactive Controller well. Moreover, this car-following model has been well calibrated, especially with respect to commercial trucks through previous studies and implemented in SwashSim (Washburn, 2024).

$$a_h(t+1) = K\frac{x_{h_+}(t) - x_h(t) - L_{h_+} - \tau_h v_h(t) + [v_h(t) - v_{h_+}(t)]\Delta t - 0.5a_{h_+}(t)\Delta t^2}{\Delta t\left(\tau_h + \frac{1}{2\Delta t}\right)} \quad (1)$$

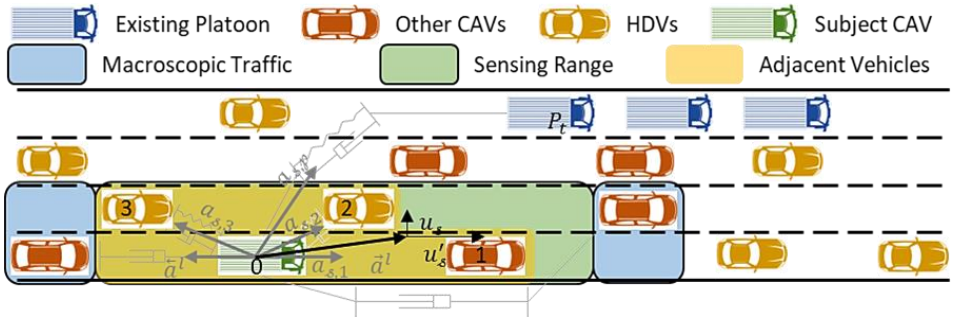

Figure 1: Representation of the traffic stream, various elements of the reactive controller.

Commented [SW12]: This material is more appropriate in the research approach section.

Commented [SW13]: I would add a separate sentence that this car-following model, as implemented in SwashSim, has been calibrated, especially with respect to commercial trucks, through previous studies (Washburn, 2024). I added the following to the references section "Washburn, S.S. *SwashSim Documentation*. 2024. https://github.com/swash17/SwashSim.

The documentation is currently at the Miraheze site, but I am going to be moving it to GitHub soon.

Commented [SW14]: Add at least half a line spacing before and after equations. I suggest using an 'equation' style for the equations and then setting the before and after paragraph spacing to 6 point.

Commented [SW15]: Some of the equations, such as this one, need the font size increased.

Commented [SW16]: See this page--https://swashsim.miraheze.org/wiki/Car_Following—for the correct formulation. The left-hand term should definitely use 'a', indicating acceleration. 'u' is often used for velocity.

Where, $a_h(t+1)$ is the modelled acceleration for the HDV h at timestep $t+1$. $x_{h_+}(t) - x_h(t) - L_{h_+}$ represents the current spacing between the HDV and its leader h_+ and $\tau_h v_h(t) + [v_h(t) - v_{h_+}(t)]\Delta t - 0.5 a_{h_+}(t)\Delta t^2$ is the target spacing. τ_h is the target headway, $v_h(t), v_{h_+}(t)$ are the velocities at timestep t. K is a sensitivity parameter analogous to a spring constant. For uninterrupted flow, $K = 0.75$. The HDVs have a constant acceleration during the timestep. Therefore, the position and velocity trajectories can be found using the double integral model in (2).

$$\begin{matrix} x_h(t+1) = x_h(t) + v_h(t) \times \Delta t + {}^1\!/_2\, u_h(t) \times \Delta t^2 \\ v_h(t+1) = v_h(t) + a_h(t) \times \Delta t \end{matrix}, t \in Z_+ \quad (2)$$

Next, the n-CAVs are considered to follow Cooperative Adaptive Cruise Control (CACC). Without loss of generality, the well-calibrated CACC scheme derived by PATH (*California Partners for advanced transportation technology* (no date)) from field data (Milanés and Shladover, 2014) is chosen.

Commented [SW17]: I assume you are referring to the group at UC Berkeley—if so, I would add a reference to their web site, just a general one, so it is clear who/what 'PATH' is.

$$\begin{matrix} e_n(t) = x_{n_+}(t) - x_n(t) - t_n v_n(t) \\ v_n(t+1) = v_n(t) + k_1 e_n(t) + k_2 \dot{e}_n(t) \end{matrix} \quad (3)$$

Where, $v_n(t+1)$ is the target velocity for the n-CAV at timestep $t+1$. e_n is the error in position and $\dot{e}_n$ is its time derivative. t_n, k_1, k_2 are tunable parameters of the system. For a car-following scheme, $k_1 = 0.45\ \mathrm{s}^{-2}, k_2 = 0.25\ \mathrm{s}^{-1}, t_n = 1\ \mathrm{s}$. CACC assumes that the vehicles have a constant velocity during a timestep. Therefore, the n-CAV's position is found using the single integral model.

$$x_n(t+1) = x_n(t) + v_n(t) \times \Delta t, \ \ t \in Z_+ \quad (4)$$

At the initial stage when StPF is activated, a CAV truck platoon may not exist in the traffic stream. Once the first platoon is formed, this approach can adapt to various platooning control schemes, such as CACC or more advanced platoon-centered control schemes (Zhang *et al*., 2022).

2.1.2 Macroscopic Traffic Characteristics

The platoon formation, if not well operated, is one of the most disruptive maneuvers to the traffic flow (Maiti *et al*., 2019, Woo and Skabardonis, 2018). To mitigate such disruption, the controller must factor in impacts on the surrounding traffic environment; that is, the distant macroscopic traffic flow, which features an aggregated traffic stream, such as density and speed. To do that, this study uses Cell Transmission Model (CTM) to mathematically capture discrete traffic evolution dynamics by dividing each road segment into road cells $c \in \mathbb{C}$ with the length L_c of each cell constrained by the Courant–Friedrichs–Lewy (CFL) condition given below.

Commented [SW18]: Only use "i.e.," or "e.g.," within parentheticals. Otherwise, spell out "that is" and "for example".

$$L_c \geq \Delta t \times v_f \quad (5)$$

Where, Δt is the uniform time interval, and v_f is the free-flow speed of the traffic stream. The evolution of the traffic density $\rho_c^l(t)$ of each cell on each lane l at timestep t is further calculated from the flow conservation law as:

$$\rho_c^l(t+1) = \rho_c^l(t) + L_c[\phi_c^l(t) - \phi_{c+1}^l(t)]/\Delta t \quad (6)$$

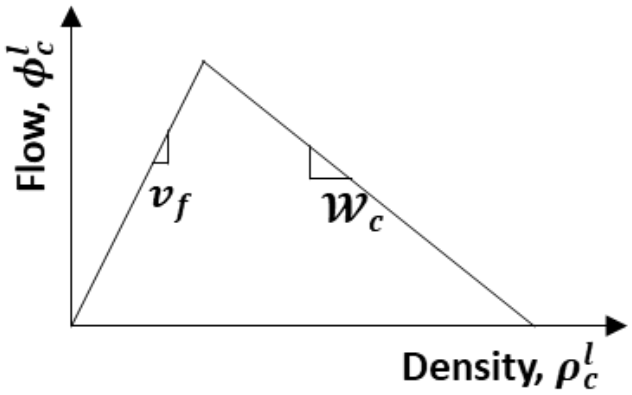

Figure 2: Fundamental Diagram

$$\phi_c^l(t) = \min[\mathcal{D}_{c-1}^l(t), \mathcal{S}_c^l(t)] \tag{7}$$

$$\mathcal{D}_c^l(t) = \min\left[v_c^l(t) \times \rho_c^l(t), \overline{q}_c\right] \tag{8}$$

$$\mathcal{S}_c^l(t) = \min\left[w_c(t) \times \left(\overline{\rho}_c - \rho_c^l(t)\right), \overline{q}_c\right] \tag{9}$$

Where, $\phi_c^l(t)$ is the traffic flow into the cell c of lane l at time t and can be calculated by the lower of the sending flow from the upstream cell $c-1, \mathcal{D}_{c-1}^l(t)$ in (8) and the receiving flow of the cell c, $\mathcal{S}_c^l(t)$ in (9). Clearly, the demand or sending flow is the number of vehicles wanting to enter the cell c at time t and it must be lesser than or equal to the capacity. The supply or receiving flow is the number of vehicles that can be accommodated by cell c at time t and is lower of the cell's available and maximum capacity ($\overline{q}_c$). The available capacity is the product of the shockwave speed ($\mathcal{W}_c$, obtained from the fundamental diagram (Figure 2) and the remaining density. Moreover, the average vehicle speed in each cell can be calculated from the fundamental equation as:

Commented [SW19]: This is hard to read. I would split out the flow-density plot as a separate figure and make both larger.

$$v_c^l(t) = \phi_c^l(t)/\rho_c^l(t) \tag{10}$$

The formulations above enable the capture of the $\mathcal{s}$-CAV's neighboring and surrounding traffic dynamics. The following section will focus on the reactive controller development for the $\mathcal{s}$-CAV to form the platoon while being aware of its traffic environment.

3.0 REACTIVE CONTROL

This section will develop the reactive controller to efficiently make an individual $\mathcal{s}$-CAV approach its target leader to form/extend a platoon without jeopardizing the safety and efficiency of its surrounding traffic. To do that, the motion of the $\mathcal{s}$-CAV considering its physical limitations is described first. Building on that, the $\mathcal{s}$-CAV's longitudinal motion and lane change control inputs are developed based on its response to its target leader, adjacent traffic, and distant macroscopic traffic flow. This is done in order to comprehensively factor the platoon formation efficiency and safety as well as their impacts on surrounding microscopic and macroscopic traffic flow. As alluded to earlier, this section assumes that the $\mathcal{s}$-CAV and its target lead truck $\mathcal{p}$ are given. Therefore, their corresponding sets are omitted to simplify the notations. The controller and the traffic environment are shown in Figure 1

3.1 DESCRIPTION OF MOTION AND CONTROL SCHEME

Vehicle movement has been described by simplified vehicle dynamics models such as the bicycle model (El Ganaoui-Mourlan *et al*., 2021, Zhang *et al*., 2022) or the double integral model (Bang *et al*., 2017, Qiu & Du, 2023) in literature. This study assumes that the acceleration remains constant during a timestep, and lane changes happen in one timestep, after checking for an available gap, allowing the use of the double integral model below to describe the longitudinal motion.

$$\begin{matrix} x_{\mathcal{s}}(t+1) = x_{\mathcal{s}}(t) + v_{\mathcal{s}}(t) \times \Delta t + {}^{1}\!/_{2}\, u_{\mathcal{s}}(t) \times \Delta t^{2} \\ v_{\mathcal{s}}(t+1) = v_{\mathcal{s}}(t) + u_{\mathcal{s}}(t) \times \Delta t \end{matrix}, \mathrm{t} \in Z_{+} \tag{11}$$

Where, $x_{\mathcal{s}}(t).\, v_{\mathcal{s}}(t).\, u_{\mathcal{s}}(t)$ represents the longitudinal position, velocity, and acceleration of the $\mathcal{s}$-CAV at time t. Physically, it relies on the tractive force (F_1) to overcome the aerodynamic (F_2) and rolling (F_3) resistances, and the grade of the road (F_4). Balancing these forces, we get:

$$m_{\mathcal{s}} u_{\mathcal{s}}(t) = F_{1,\mathcal{s}}(t) - F_{2,\mathcal{s}}(t) - F_{3,\mathcal{s}}(t) - F_{4,\mathcal{s}}(t), \mathrm{t} \in Z_{+} \tag{12}$$

The maximum tractive force $\overline{F}_1(t)$ is assumed to be known, which is dependent on $\mathcal{s}$-CAV's current powertrain state, is known. Therefore, the $\mathcal{s}$-CAV's maximum possible acceleration at every timestep, $\bar{a}_{\mathcal{s}}(t)$ can be calculated as:

$$m_{\mathcal{s}} \bar{a}_{\mathcal{s}}(t) = \overline{F}_{1,\mathcal{s}}(t) - F_{2,\mathcal{s}}(t) - F_{3,\mathcal{s}}(t) - F_{4,\mathcal{s}}(t), \mathrm{t} \in Z_{+} \tag{13}$$

The reactive controller will therefore calculate the control input as a fraction of the maximum acceleration of the current state, while responding to its target leader, indexed by $\mathcal{p}$, the set of adjacent vehicles, indexed by $\mathbb{A} \in \Omega_{\mathbb{A}}(t)$ and the macroscopic upstream and downstream traffic, accented by $\leftarrow$ and $\rightarrow$ in the respective lane. Then, the acceleration and relative alignment vectors

are represented by the s-CAV's responses to the target leader, adjacent vehicles, and upstream and downstream traffic.

$$a(t) = \left[a_p(t), a_{\mathbb{A}}(t), \tilde{a}^l(t), \vec{a}^l(t)\right], \mathbb{A} \in \Omega_{\mathbb{A}}(t), l \in \mathbb{L}, t \in Z_+$$
$$\theta(t) = \left[\theta_p(t), \theta_{\mathbb{A}}(t), \tilde{\theta}^l(t), \vec{\theta}^l(t)\right], \mathbb{A} \in \Omega_{\mathbb{A}}(t), l \in \mathbb{L}, t \in Z_+$$

Finally, it is converted to the control input as $u_s(t) = f(a(t), \theta(t), \bar{a}_s)$. The discussions on the calculations of the acceleration and alignment vectors and conversion to the control inputs is presented in the next sections.

3.2 REACTION TO THE TARGET LEADER BY SPRING-MASS-DAMPER

This reactive controller seeks to drive the s-CAV to approach its target leader p on a different lane with a safe car-following distance. To facilitate the catch-up maneuver, a virtual spring-mass-damper (SMD) link is created between the s-CAV and its target leader. The spring is featured by a spring function $F^s_{s,p}(t)$, length $\mathcal{L}_{s,p}(t)$, and natural resting length $\ell_{s,p}(t)$ will push the s-CAV toward its target leader, while the damper described by a damper function $F^d_{s,p}(t)$ will match their velocities. The s-CAV has a virtual mass m_s.

To allow for a rapid approach, the s-CAV should maintain a constant and high acceleration as it catches up to its leader. Once it gets close, the acceleration should transition to a linear function to facilitate finer control and allow for precise maneuvering. If the lead vehicle is identified at the upper limit of the sensing/communication range, the acceleration should increase smoothly. It is imperative that the transition between the states is smooth in order to ensure passenger comfort. To address these special requirements, this study designs the spring following a nonlinear model defined by (14) and visualized in Figure 3.

$$F^s_{s,p}(t) = \tanh\left(\alpha_1 \Delta x_{s,p}(t)\right) \tag{14}$$

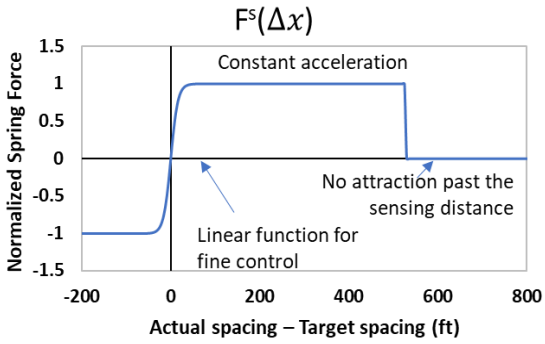

Figure 3: Spring function.

$$\Delta x_{s,p}(t) = \mathcal{L}_{s,p}(t) - \ell_{s,p}(t) \quad (15)$$

Commented [SW20]: I would make these separate figures and enlarge. Two small when side-by-side.

Where, $\Delta x_{s,p}(t)$ is the stretch in the spring and x_b is the breakoff distance where the attraction diminishes and represents the communication range, which is about 1000 ft. α_1 is a tunable coefficient between 0 and 1 that defines the curvatures of the force function near the ideal following distance. Larger α_1 allows the spring function to achieve the maximum force at a shorter stretch at the expense of stability issues. Smaller α_1 provides finer control for longer but results in a slower catch-up. The natural resting length of the link is the ideal car-following distance between the two vehicles. There are multiple variations of the ideal car-following distance developed in literature and it is not the focus of this study. Therefore, without the loss of generality, the ideal car-following distance developed by Gong & Du, (2018) which ensures conflict-free driving is chosen.

$$\ell_{s,p}(t) = L_s + \tau_{s,p} v_s(t) + v_s(t)^2/2b_s - v_p(t)^2/2b_p \quad (16)$$

Where L_s is the length of the s-CAV, $\tau_{s,p}$ is target headway and $v_s(t)^2/2b_s$, $v_p(t)^2/2b_p$ represents the braking distance of the s-CAV and the target leader. The actual gap is the bumper-bumper distance given by:

$$\mathcal{L}_{s,p}(t) = x_p(t) - L_p - x_s(t) \quad (17)$$

Similarly, a non-linear damper is defined in (18) that allows the s-CAV to reduce a large relative velocity at a constant acceleration and transition smoothly to a linear function when it becomes small enough to allow precise control. The damper function is visualized in Figure 4.

Commented [SW21]: Fix link.

$$F^d_{s,p}(t) = \tanh\left(\alpha_3 \Delta v_{s,p}(t)\right) \quad (18)$$

$$\Delta v_{s,p}(t) = v_p(t) - v_s(t) \quad (19)$$

Where, $\Delta v_{s,p}(t)$ is the relative velocity between the target leader and the s-CAV. α_3 defines the curvature at 0 relative velocity and takes any value between 0 and 1. The optimal value should give a good balance between the linear and nonlinear parts of the damper force. It is related to the

Commented [SW22]: Better to use 'mi/h', rather than 'mi/hr' (x-axis label in Fig. 4).

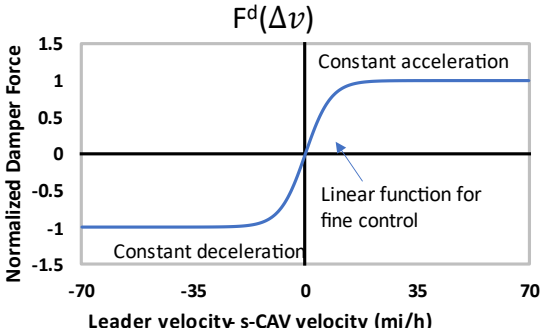

Figure 4: Damper function.

spring parameter α_1 through the damping ratio and will be discussed in Section 3.5. The relative alignment $\theta_{s,\mathcal{P}}(t)$ is found using trigonometry and the resultant acceleration $a_{s,\mathcal{P}}(t)$ produced in this virtual link is found using force balance.

$$a_{s,\mathcal{P}}(t) = \left(F^{s}_{s,\mathcal{P}}(t) + F^{d}_{s,\mathcal{P}}(t)\right)/m_s \tag{20}$$

$$\theta_{s,\mathcal{P}}(t) = \tan^{-1}\left[n_{s,\mathcal{P}}(t) \times w/\mathcal{L}_{s,\mathcal{P}}(t)\right] \tag{21}$$

Where, $n_{s,\mathcal{P}}(t)$ is the number of lanes between the s-CAV and the target leader and w is the lane width. This study sets the lane width to be 12 ft, per AASHTO Guidelines.

3.3 REACTION TO THE TARGET LEADER BY SPRING-MASS-DAMPER

The s-CAV must catch up to its target leader while avoiding collision with its adjacent vehicles and interrupting their mobility. To do this, it is assumed that the s-CAV uses onboard or roadside sensors to detect its surrounding vehicles in adjacent lanes. According to existing studies, the sensors to have a limited range x_b (e.g., 650 ft). All the vehicles within the sensing distance are added to the Adjacent Vehicles set $\Omega_{\mathbb{A}}(t)$ and virtual SMD links are created for the s-CAV to respond to every adjacent vehicle in $\Omega_{\mathbb{A}}(t)$ at every timestep to avoid collision. The actual ($\mathcal{L}_{s,\mathbb{A}}(t)$) and the natural resting length ($\ell_{s,\mathbb{A}}(t)$) of each SMD link is dependent on the position of the s-CAV and is defined as:

$$\mathcal{L}_{s,\mathbb{A}}(t) = \begin{cases} x_{\mathbb{A}}(t) - L_{\mathbb{A}} - x_s(t) & \text{if } x_{\mathbb{A}}(t) > x_s(t) \\ x_s(t) - L_s - x_{\mathbb{A}}(t) & \text{if } x_{\mathbb{A}}(t) < x_s(t) \end{cases}, \mathbb{A} \in \Omega_{\mathbb{A}}(t) \tag{22}$$

$$\ell_{s,\mathbb{A}}(t) = \begin{cases} L_s + \tau_{s,\mathbb{A}} v_s(t) + v_s(t)^2/2b_s - v_{\mathbb{A}}(t)^2/2b_{\mathbb{A}} & \text{if } x_{\mathbb{A}}(t) > x_s(t) \\ L_s + \tau_{s,\mathbb{A}} v_s(t) + v_{\mathbb{A}}(t)^2/2b_{\mathbb{A}} - v_s(t)^2/2b_s & \text{if } x_{\mathbb{A}}(t) < x_s(t) \end{cases}, \mathbb{A} \in \Omega_{\mathbb{A}}(t) \tag{23}$$

The spring force ($F^{s}_{s,\mathbb{A}}(t)$) can be calculated by plugging $\Delta x_{s,\mathbb{A}}(t) = \mathcal{L}_{s,\mathbb{A}}(t) - \ell_{s,\mathbb{A}}(t)$ in (14). The relative velocity depends on the s-CAV's position and is defined as:

$$\Delta v_{s,\mathbb{A}}(t) = \begin{cases} v_{\mathbb{A}}(t) - v_s(t) & \text{if } x_{\mathbb{A}}(t) > x_s(t) \\ v_s(t) - v_{\mathbb{A}}(t) & \text{if } x_{\mathbb{A}}(t) < x_s(t) \end{cases}, \mathbb{A} \in \Omega_{\mathbb{A}}(t) \tag{24}$$

The damper force ($F^{d}_{s,\mathbb{A}}(t)$) can be calculated by plugging $\Delta v_{s,\mathbb{A}}(t)$ in (18). Then, the reaction to every adjacent vehicle and the relative orientation is calculated as:

$$a_{s,\mathbb{A}}(t) = \left(F^{s}_{s,\mathbb{A}}(t) + F^{d}_{s,\mathbb{A}}(t)\right)/m_s\,, \mathbb{A} \in \Omega_{\mathbb{A}}(t) \tag{25}$$

$$\theta_{s,\mathbb{A}}(t) = \begin{cases} \tan^{-1}\left[n_{s,\mathbb{A}}(t) \times w/\mathcal{L}_{s,\mathbb{A}}(t)\right] & \text{if } x_{\mathbb{A}}(t) > x_s(t) \\ \tan^{-1}\left[n_{s,\mathbb{A}}(t) \times w/\mathcal{L}_{s,\mathbb{A}}(t)\right] + 180° & \text{if } x_{\mathbb{A}}(t) < x_s(t) \end{cases}, \mathbb{A} \in \Omega_{\mathbb{A}}(t) \tag{26}$$

3.4 REACTION TO DISTANT TRAFFIC

The platoon formation process must hold the following two merits: (i) not causing severe traffic fluctuations that propagate upstream and (ii) responding to the variations in downstream traffic conditions to improve platoon formation efficiency; for example, choosing a lane with relatively sparse traffic to form the platoon. To do these, design additional virtual SMD links that respond to the upstream and downstream macroscopic traffic conditions are designed. These macroscopic traffic conditions can be tracked using the CTM introduced in (6)-(10) with the boundary and initial conditions observed by various V2X technologies at each timestep. However, to capture the impact of $\mathcal{s}$-CAV's movement on distant traffic, the interaction between $\mathcal{s}$-CAV's adjacent microscopic flow and the distant macroscopic flows still needs to be captured. Namely, a vehicle in the adjacent vehicles set $\Omega_{\mathbb{A}}(t)$ at timestep t may move away and be aggregated as a part of the macroscopic traffic and vice versa by responding to motion of the $\mathcal{s}$-CAV and/or general traffic dynamics.

To identify this micro- and macro- traffic interaction, the interaction zone is defined as the region that affects/is affected by the movement of the $\mathcal{s}$-CAV in one timestep. To be noted, this zone is not stationary, and its length depends on the traffic flow dynamics. The disturbance created by the $\mathcal{s}$-CAV to its adjacent vehicles will propagate upstream or downstream as a shockwave with the speeds calculated by (25) through the interaction zone.

$$\begin{matrix} \overrightarrow{w}_{c_s}(t) = \left(\phi_{c_s}(t) - \phi_{\vec{c}}(t)\right)/\left(\rho_{c_s}(t) - \rho_{\vec{c}}(t)\right) \\ \overleftarrow{w}_{c_s}(t) = \left(\phi_{c_s}(t) - \phi_{\overleftarrow{c}}(t)\right)/\left(\rho_{c_s}(t) - \rho_{\overleftarrow{c}}(t)\right) \end{matrix}, \forall\, t \in Z_+ \tag{27}$$

Where c_s is the segment containing the $\mathcal{s}$-CAV and its adjacent vehicles, $\overleftarrow{c}$ and $\vec{c}$ are the CTM cells containing the downstream and upstream interaction zones, respectively. Their length can be calculated by:

$$\begin{matrix} \Delta\vec{x}(t) = \overrightarrow{w}_{c_s}(t) \times \Delta t \\ \Delta\overleftarrow{x}(t) = \overleftarrow{w}_{c_s}(t) \times \Delta t' \end{matrix} \forall\, t \in Z_+ \tag{28}$$

Given the length of a CTM cell is also constrained by the CFL condition in (5), the interaction zones will be constrained within one CTM cell each since the shockwave speed will always be less than or equal to the free flow traffic speed. The micro- macro- interaction zones consisting of $\overleftarrow{c}, \vec{c}$ and the segment c_s is visualized in Figure 1. The segment c_s contains the $\mathcal{s}$-CAV and its adjacent vehicles and its boundary and length are given below.

$$\begin{matrix} \overline{x}_{c_s}(t) = x_s(t) + x_b \\ \underline{x}_{c_s}(t) = x_s(t) - L_s - x_b \\ L_{c_s} = \overline{x}_{c_s}(t) - \underline{x}_{c_s}(t) = L_s + 2x_b \end{matrix} \tag{29}$$

The $\mathcal{s}$-CAV can sense the position and velocity of each vehicle in cell c_s and their position and velocity can be predicted by using (1)-(4). Therefore, the density per lane of c_s can be measured by (30) at the current timestep and be estimated for the next timestep.

$$\rho_{c_s}^l(t) = \sum_{\omega \in \Omega(t)} \lambda_{\omega,c_s}^l(t) / \Delta L_{c_s}, \forall\, l \in \mathbb{L}, t \in Z_+ \tag{30}$$

Where, $\lambda_{\omega,c_s}^l(t) = 1$ if vehicle ω is in lane l of cell c at time t and is used to identify the cell and lane of the $\mathcal{s}$-CAV and its adjacent vehicles. Using this density, the flow propagation $(\phi_{c_s}(t), \phi_{\vec{c}}(t))$ among cells can be captured by (7)-(9) and the density evolution can be calculated using (6). The average speed in the interaction zones can be calculated from the fundamental equation using (10).

The impacts of the $\mathcal{s}$-CAV's movement on the interaction zone in one timestep is counted in the next time in this discrete control. To do this, the location of the adjacent vehicles and $\mathcal{s}$-CAV are predicted for the next timestep using (1)-(4), (11), (34) and the same procedure described above (27)-(30) can be repeated to estimate the average speed in the interaction zones in the next timestep $(\tilde{v}^l(t+1),\ \vec{v}^l(t+1))$. Finally, the impact of the $\mathcal{s}$-CAV on the macroscopic traffic can be quantified as the difference in average speed of the cells between two timesteps.

$$\begin{matrix} \Delta\tilde{v}^l(t) = \tilde{v}^l(t) - \tilde{v}^l(t+1) \\ \Delta\vec{v}^l(t) = \vec{v}^l(t) - \vec{v}^l(t+1) \end{matrix}, \forall\, l \in \mathbb{L}, t \in Z_+ \tag{31}$$

A positive $\Delta\tilde{v}^l(t)$ or $\Delta\vec{v}^l(t)$ means the $\mathcal{s}$-CAV's movement will slow macroscopic traffic in the next timestep and is undesirable. To compensate for this, dampers are added between the $\mathcal{s}$-CAV and the interaction zones. By plugging in the relative velocities calculated in (29) in (17), the damper forces $\tilde{F}_d^l$ and $\vec{F}_d^l$ are obtained. The relative alignment and the acceleration due to these forces are:

$$\begin{matrix} \vec{\theta}^l(t) = \tan^{-1}\left[n_{s,l}(t) \times w / \underline{x}_{c^+}(t) - x_s(t)\right] \\ \tilde{\theta}^l(t) = \tan^{-1}\left[n_{s,l}(t) \times w / x_s(t) - \overline{x}_{c^-}(t)\right] \end{matrix}, \forall\, l \in \mathbb{L}, t \in Z_+ \tag{32}$$

$$\begin{matrix} \vec{a}^l(t) = \vec{F}_d^l(t) / m_s \\ \tilde{a}^l(t) = \tilde{F}_d^l\,(t) / m_s \end{matrix}, \forall\, l \in \mathbb{L}, t \in Z_+ \tag{33}$$

The above formulations (11) to (33) respectively calculate the $\mathcal{s}$-CAV's responses to its target leader, adjacent vehicles, and distant upstream and downstream traffic.

3.5 OUTPUT OF THE REACTIVE CONTROLLER

This section demonstrates how to comprehensively use the reactive accelerations obtained in the above sections to control the $\mathcal{s}$-CAV's longitudinal and lateral movement during platoon formation in this complicated traffic environment. Specifically, the $\mathcal{s}$-CAV's longitudinal motion follows the double integral model described in (11), which is built upon the longitudinal acceleration $u_s(t) = f(a(t), \theta(t), \bar{a}_s)$. The accelerations calculated in the previous sections $a(t) = \left[a_{\mathcal{p}}(t), a_{\mathbb{A}}(t), \tilde{a}^l(t), \vec{a}^l(t)\right]$ must be resolved to their longitudinal and lateral components by their relative alignment $\theta(t) = \left[\theta_{\mathcal{p}}(t), \theta_{\mathbb{A}}(t), \tilde{\theta}^l(t), \vec{\theta}^l(t)\right]$. The lateral components will determine the lane changes.

Tunable weights $\beta_1, \beta_2, \beta_3$, satisfying $\beta_i \geq 0, \sum_i \beta_i = 1$ are defined for each of the three types of SMD links. β_1 is the weight for the link between the $\mathcal{s}$-CAV and the target leader and prioritizes platoon formation efficiency. β_2 is the weight for the links between the $\mathcal{s}$-CAV and its adjacent vehicles and secures traffic safety. β_3 is the weight for the links between the $\mathcal{s}$-CAV and the macroscopic traffic and ensures traffic efficiency. The weights determine the priority of their corresponding response and their effects will be demonstrated through sensitivity tests. Then, the net longitudinal acceleration in (34) is scaled by the $\mathcal{s}$-CAV's maximum acceleration (13).

$$u_{\mathcal{s}}(t) = \bar{a}_{\mathcal{s}}(t) \times \max\left\{\begin{pmatrix} \beta_1 \times a_{\mathcal{s},\mathcal{p}}(t) \times \cos(\theta_{\mathcal{s},\mathcal{p}}(t)) + \\ \beta_2 \times \sum_{\mathbb{A}} (a_{\mathcal{s},\mathbb{A}}(t) \times \cos(\theta_{\mathcal{s},\mathbb{A}}(t))) + \\ \beta_3 \times \sum_l (\vec{a}^l(t) \times \cos(\vec{\theta}^l(t)) + \overleftarrow{a}^l(t) \times \cos(\overleftarrow{\theta}^l(t))) \end{pmatrix}, 1\right\} \quad (34)$$

The net lateral acceleration in (33) serves as the motivation for lane change as needed for the platoon formation.

$$u'_{\mathcal{s}}(t) = \bar{a}_{\mathcal{s}}(t) \times \max\left\{\begin{pmatrix} \beta_1 \times a_{\mathcal{s},\mathcal{p}}(t) \times \sin(\theta_{\mathcal{s},\mathcal{p}}(t)) + \\ \beta_2 \times \sum_{\mathbb{A}} (a_{\mathcal{s},\mathbb{A}}(t) \times \sin(\theta_{\mathcal{s},\mathbb{A}}(t))) + \\ \beta_3 \times \sum_l (\vec{a}^l(t) \times \sin(\vec{\theta}^l(t)) + \overleftarrow{a}^l(t) \times \sin(\overleftarrow{\theta}^l(t))) \end{pmatrix}, 1\right\} \quad (35)$$

A positive value of $u'_{\mathcal{s}}(t)$ indicates the $\mathcal{s}$-CAV wants to switch to an outer lane, while a negative value indicates the $\mathcal{s}$-CAV wants to switch to an inner lane. These lane changes, which are discretionary in nature, are executed according to the following the two conditions.

- First, the $\mathcal{s}$-CAV must be attracted to (or repelled by) an adjacent lane with sufficient motivation; that is, an acceleration greater than a threshold, $\overline{u}'_{\mathcal{s}}$. A low threshold allows earlier lane changes but may also have the $\mathcal{s}$-CAV frequently oscillate between lanes, which would risk traffic safety and degrade occupants' comfort. A high threshold makes the $\mathcal{s}$-CAV too conservative to change lanes and lose opportunities to form a platoon on a sparse lane.

- Second, both the lead and lag gaps in target lane must be acceptable for safety consideration (Ahmed, 1999). Following this thought, the spring connecting to the adjacent vehicles must be stretched for a gap to be acceptable. Let $\mathbb{A}_-, \mathbb{A}_+ \in \Omega_{\mathbb{A}}(t)$ be the lead and lag vehicles in the target lane that the $\mathcal{s}$-CAV wants to change to. If $\mathcal{L}_{\mathcal{s},\mathbb{A}_+}(t) > \ell_{\mathcal{s},\mathbb{A}_+}(t) \wedge \mathcal{L}_{\mathcal{s},\mathbb{A}_-}(t) > \ell_{\mathcal{s},\mathbb{A}_-}(t)$, the gap is acceptable. If both conditions are satisfied, then a lane change request is granted to the $\mathcal{s}$-CAV and will be executed in the current timestep. The catch-up maneuver is completed when the $\mathcal{s}$-CAV is in the same lane as its target leader, their gap is the same as the ideal following distance and have the same speed; that is, $n_{\mathcal{s},\mathcal{p}}(t) = 0, \mathcal{L}_{\mathcal{s},\mathcal{p}}(t) = \ell_{\mathcal{s},\mathcal{p}}(t), \Delta v_{\mathcal{s},\mathcal{p}}(t) = 0$. In this state, the platoon will absorb the $\mathcal{s}$-CAV and will switch to the control scheme described earlier.

Commented [SW23]: Should the "=" at the end be deleted?

The SMD-based Reactive Controller needs to transition smoothly between different equilibrium points under dynamic traffic conditions. The smooth spring and damper functions enable the resultant forces to push the $\mathcal{s}$-CAV towards the dynamic equilibrium. The damping ratio of the spring and damper dictates the efficiency of this motion. Over-damped systems take longer to

approach the equilibrium point, while under-damped systems approach the equilibrium point faster but oscillate around it, which causes discomfort and is unsafe. Theoretical analysis showed that for the customized spring and damper functions, the most efficient and safe way to reach equilibrium can be achieved under the critical damping ratio by setting $\alpha_1 = \bar{a}_s {\alpha_3}^2/4$.

4.0 SEQUENTIAL TRUCK PLATOON FORMATION ALGORITHM

As mentioned in the problem statement, there may multiple $\mathcal{s}$-CAVs within the communication range of each other willing to form/join the platoon at any timestep ($\Omega_{\mathcal{s}}(t)$). This situation calls for an algorithm that can manage those requests to form platoons efficiently, while mitigating negative traffic impacts. Given truck platoon formation and their associated movements are prone to cause significant traffic safety concerns, this study proposes a Sequential truck Platoon Formation algorithm (StPF) that sequentially feeds the reactive controller with the next $\mathcal{s}$-CAV $\mathcal{s}(t)$ and its target leader $\mathcal{p}(t)$ to satisfy the platoon formation requests from multiple trucks. To develop this algorithm, the set $\mathbb{P}(t)$ that contains the trucks in the formed platoon is utilized. Below, the key ideas of the algorithm are introduced and its two unique and enhanced features are highlighted. StPF will start with the most downstream pair as the leader (using (36)) and the follower (using (37)) and form the first two-vehicle platoon.

$$\mathcal{p}(t) \coloneqq \text{argmin}_p\{x_p(t), p \in \mathbb{P}(t)\};\ \mathbb{P}(0) \coloneqq \text{argmax}_\omega\ \{x_\omega(0), \forall \omega \in \Omega_{\mathcal{s}}(0)\} \quad (36)$$

$$\mathcal{s}(t) \coloneqq \text{argmax}_\omega\ \{x_\omega(t), \forall \omega \in \Omega_{\mathcal{s}}(t) \setminus \mathcal{p}(t)\} \quad (37)$$

Commented [SW24]: Are the colons necessary before the "≔" in the equations on this page?

Commented [MN25R24]: Since they are used as set definitions here, yes.

Once the platoon is formed, $\mathcal{s}(t)$ will be added to $\mathbb{P}(t)$. StPF will sequentially add the next most downstream $\mathcal{s}$-CAV to the platoon by assigning its most upstream truck in the platoon as its target leader. This procedure will be repeated until all the $\mathcal{s}$-CAV's within the communication range has been added to the platoon.

StPF is further enhanced to compensate for non-cooperative HDVs following the target leader, blocking the platoon formation. To enable this, the current $\mathcal{s}$-CAV is allowed to follow a proxy leader by examining the vehicle immediately upstream of the target leader (38).

$$\mathcal{p}^-(t) \coloneqq \{\omega: (x_{\mathcal{p}}(t) - x_\omega(t) < x_{\mathcal{p}}(t) - x_{\omega'}(t)), \forall \omega \in \Omega(t), \omega' \in \Omega(t) \setminus \omega, l \in \mathbb{L}\} \quad (38)$$

If the immediate vehicle behind the target leader is the $\mathcal{s}$-CAV that needs to join the platoon, then there is no need for any adjustment. Otherwise, if the gap between the target leader and its immediate upstream vehicle is smaller than the ideal following distance for the $\mathcal{s}$-CAV, it would not be able to cut in front of this vehicle. Therefore, this vehicle will be deemed to be a non-HDV and will be selected as the proxy target leader, using (39).

$$\mathcal{p}(t) \coloneqq \begin{cases} \mathcal{p}(t) & \text{if } \mathcal{L}_{\mathcal{p}^-,\mathcal{p}}(t) > \ell_{\mathcal{p}^-,\mathcal{p}}(t) \\ \mathcal{p}^-(t) & \text{otherwise} \end{cases} \quad (39)$$

Where, $\mathcal{L}_{\mathcal{p}^-,\mathcal{p}}(t)$ is the actual bumper-bumper gap and $\ell_{\mathcal{p}^-,\mathcal{p}}(t)$ represents the ideal following distance. Without the loss of generality, it can be assumed to follow equations (16, 17), by plugging in $\mathcal{p}^-$ instead of $\mathcal{s}$.

Furthermore, this StPF algorithm allows the formation of multiple platoons in different positions of the freeway simultaneously, when the $\mathcal{s}$-CAVs clusters (such as Ω_s^1, Ω_s^2, etc.) are outside the communication range of each other. If a short platoon approaches another one, StPF can connect them to form one long platoon. The algorithm can be further extended to simultaneous platoon formation (SiPFA) which will be more suited to cars and other light vehicles, which cause lower disruption to traffic during the platoon formation process.

5.0 EXPERIMENTS

This study conducts numerical experiments to demonstrate the effectiveness of the reactive controller and StPF. The experiments will show the importance of reacting to macroscopic traffic and identify traffic conditions where platoon formation is successful. Numerical experiments were performed on the traffic micro-simulation tool SwashSim (SwashSim, 2024). A straight 3-lane 10-mi freeway segment was set up without branches. The input flow rate and the vehicle mix were varied based on Vehicle Class History and Hourly Continuous Count data for various Telemetered Traffic Monitoring Sites on I-75 taken from the Florida Department of Transportation's Florida Traffic Online website (Florida traffic online, n.d.). All experiments were run on an Acer laptop with Intel Core i7–7700HQ CPU with 4 cores running at 2.8GHz and 16 GB RAM in Windows.

5.1 SIGNIFICANCE OF RESPONDING TO MACROSCOPIC TRAFFIC

The experiments were conducted with an input flow rate of 1500 veh/h and a vehicle mix of 28% light passenger vehicles (sedan, hatchback), 42% heavy passenger vehicles (pickup trucks and SUVs), 5% single unit trucks (SUTs), and 25% large trucks, half of which are willing to form platoons. Response to the macroscopic traffic was studied by varying $\beta_1, \beta_2, \beta_3$. Therefore, the other parameters were set to their optimum value: $\alpha_1 = 0.25, \alpha_3 = 1, \overline{u}'_s = 0.025$. To highlight the importance of responding to macroscopic traffic, the following three combinations are illustrated.

- Uniform reaction: $\beta_1 = \beta_2 = \beta_3 = 1/3$
- No response to macroscopic traffic: $\beta_1 = \beta_2 = 1/3, \beta_3 = 0$
- Best combination: $\beta_1 = 1/4, \beta_2 = 1/2, \beta_3 = 1/4$

Our experiment results showed that over a 10-minute period, 15 and 14 platoons were successfully formed when using $\beta_1 = 1/4$, $\beta_2 = 1/2$, $\beta_3 = 1/4$ and $\beta_1 = \beta_2 = \beta_3 = 1/3$ respectively, while only 8 platoons were formed with $\beta_1 = \beta_2 = 1/2$, $\beta_3 = 0$, half of which are formed by catching up to the leader on the same lane and no non-cooperating vehicles (simple catch-up). Therefore, it is claimed that accounting for the macroscopic traffic enabled the s-CAV to maintain a high speed (safely, relative to the surrounding traffic), find proper gaps to perform lane changes, and expedite platoon formation.

Commented [SW26]: Were these all pickup trucks, or a mix of SUVs and pickups?

Commented [MN27R26]: Yes.

Commented [SW28]: How high?

More interestingly, it often enabled the $\mathcal{S}$-CAV to get ahead of its target platoon leader and ultimately lead a platoon with a higher speed. These can be visualized in Figure 5. Vehicle 199 (yellow box) entered the communication range of Vehicle 192 (red box) in Figure 5a and began to catch up to it. Without reaction to the macroscopic traffic (Figure 5b), it could not find a gap to enter the middle lane and was stuck in the right lane. However, reacting to the downstream traffic (Figure 5c) allowed it to accelerate and find a gap to enter the middle lane. This reaction can be seen in Figure 6. The $\mathcal{S}$-CAV maintained its speed (solid purple line) despite the adjacent vehicles slowing down at 685 s, seen as the drop in the average speed in the cell $c_{\mathcal{S}}$ (solid yellow line). Without this reaction, the $\mathcal{S}$-CAV slowed down (dashed purple line) to match the speed of its adjacent vehicles (dashed yellow line), resulting in a negative feedback loop, and making the $\mathcal{S}$-CAV a moving bottleneck. By responding to the surrounding traffic, the $\mathcal{S}$-CAV moved faster than its surrounding traffic and could complete the catch-up to its target leader in less than 120 s. Finally, when the entry flow rate was doubled to 3000 veh/h (Figure 5d), Vehicle 199 was in the faster (right) lane. The attraction to the downstream traffic was greater than to its target leader (not shown in Figure 6), therefore Vehicle 199 gets ahead of Vehicle 192 and swaps role to be the target leader. Vehicle 192 was later able to successfully catch up to Vehicle 199.

Commented [SW29]: Catch up to what?

Commented [SW30]: Use "h" for the unit "hour".

Commented [SW31]: I would clarify whether this lane is the left, middle, or right lane.

Commented [SW32]: Therefore Vehicle 199 gets ahead…?

Commented [MN33R32]: Yes. I have clarified it.

Commented [SW34]: Define 'it'.

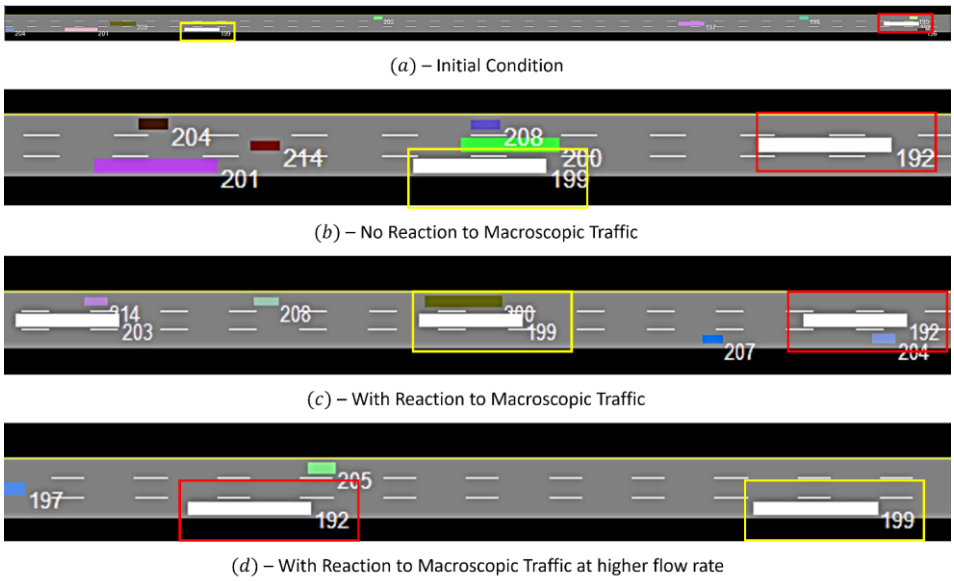

(a) – Initial Condition

(b) – No Reaction to Macroscopic Traffic

(c) – With Reaction to Macroscopic Traffic

(d) – With Reaction to Macroscopic Traffic at higher flow rate

Figure 5: Benefits of responding to the macroscopic traffic.

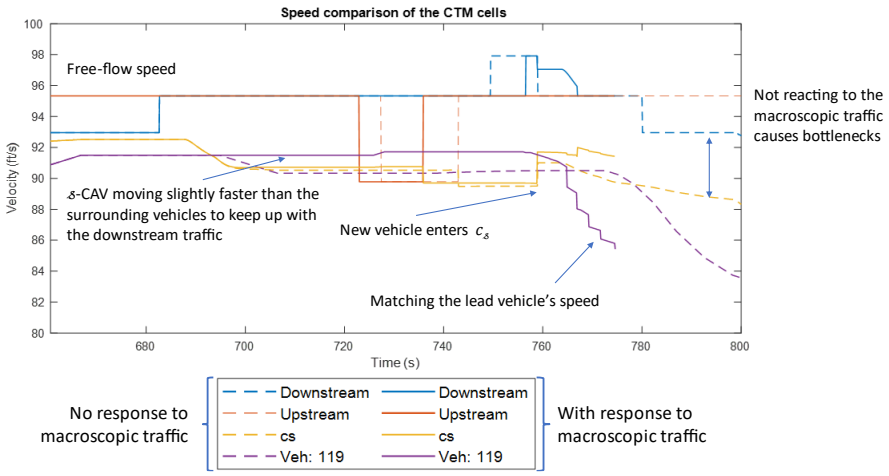

Figure 6: Speed of $\mathcal{S}$-CAV and the CTM cells during platoon formation.

These results confirmed the significance of reacting to macroscopic traffic. According to this result, the weights are chosen to be $\beta_1 = 1/4, \beta_2 = 1/2, \beta_3 = 1/4$ in the rest of the experiments.

Commented [SW35]: A ")" is missing at the end of the y-axis label for Fig. 6.

Commented [SW36]: The legend at the bottom needs to be larger.

5.2 MACROSCOPIC TRAFFIC FAVORING PLATOON FORMATION

This section attempts to identify macroscopic conditions that are favorable for truck platoon formation. The freeway configuration (3 lanes, 65 mi/h free-flow speed) and the vehicle type mix were retained from the previous section while the input flow rate was varied from 1500 veh/h to 5400 veh/h. At an input flow rate of 1500 veh/h, the average density was about 10 mi/h/ln, which

Commented [SW37]: Figure 7 is displayed before Figure 6.

Commented [SW38]: Again, split these out as separate figures and enlarge both.

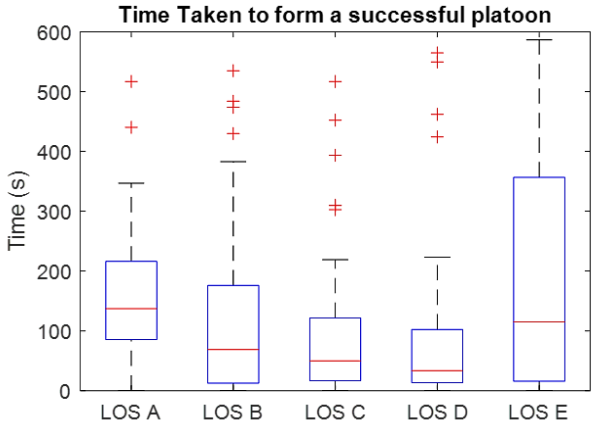

Figure 7: Time taken to form a platoon under various traffic conditions.

corresponds to a Level of Service of A (LOS A) while the average density at input flow rate of 5400 veh/h was about 44.5 veh/mi/ln, which corresponds to LOS E.

The results indicated that the time taken to form platoons decreased up to LOS C, as the surrounding flow assisted the catch-up. In these conditions, the median flow rate in the cell c_s was greater than the input flow rate (see Figure 7). Beyond LOS C, the opportunity to make lane changes reduced due to the higher density condition, leading to the only type of platoons that were formed being simple catch-up type platoons. Therefore, even though the time taken to form a platoon was low, the number of successful platoon formations was also low. Furthermore, the flow rate surrounding the s-CAV was much lower than the average input flow rate (see Figure 8). It caused the s-CAV to function as a bottleneck and led to traffic congestion. Therefore, the above experiments demonstrated that LOS C (i.e., a density of approximately 23.4 veh/mi/ln) served as the upper limit of favorable conditions for platoon formation.

Commented [SW39]: Should the units for the y-axis (Fig. 8) be "veh/h/ln"?

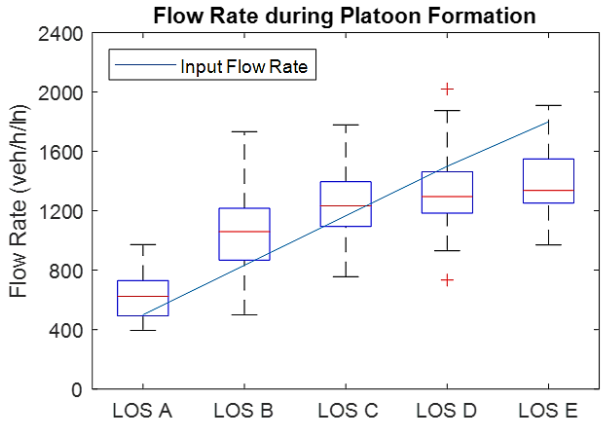

Figure 8: Flow rate around the s-CAV during platoon formation.

6.0 CONCLUSION

This project resulted in the development of the StPF algorithm, which is designed to form CAV platoons in a dynamic and mixed environment that adaptively chooses the platoon leader and the target platoon lane by actively responding to the surrounding traffic conditions. The StPF algorithm is built upon a Reactive Controller that responds to the target leader and surrounding micro- and macro- traffic by modeling their interactions as a Spring-Mass-Damper system with unique non-linear springs and dampers. Experiments conducted on a micro-simulation tool explored optimal parameter settings for the Reactive Controller and validated the StPF algorithm's effectiveness. Mainly, the experiments confirmed that responding to complicated adjacent microscopic and macroscopic traffic will enhance platoon-forming opportunities and mitigate its negative traffic impacts. The experiment results also indicated that platoon formation was generally favorable in high truck mix, high CAV penetration, and up to LOS C conditions, whereas both mildly congested and low connected truck percentage conditions inhibit platoon formation. Future work will explore the Simultaneous Platoon Formation Algorithm (SiFPA) that will be tailored for passenger vehicles. Additionally, further experiments will be conducted to quantify the travel time benefits for an individual vehicle as well as the traffic stream by enabling platoon formation. Finally, theoretical analysis must be conducted to identify the conditions necessary for guaranteeing platoon formation.

The methodological contributions of this work are summarized as follows. First, to enable StPF, a novel Reactive Controller was developed to manage trucks' longitudinal (car-following) and lateral (lane change) movements and proactively responds to the target leader for efficient catch-up while also reacting to adjacent traffic on multiple lanes and far-away traffic to ensure anti-collision behavior and traffic smoothness. Next, the StPF algorithm built upon the Reactive Controller was developed with the following enhanced features. It can adaptively determine the order of vehicles forming/joining the platoon as well as the target lane by reacting to real-time surrounding micro- and macro- traffic conditions. The adaptive order determination also allows StPF to merge two short platoons into a large one. It can also accommodate any groups of non-cooperative HDVs that prevent the formation of a pure CAV platoon by identifying and choosing an appropriate proxy HDV target leader. Finally, the performance of the algorithm and controller was evaluated using numerical experiments, suggested various traffic conditions that are favorable for platoon formation, and outlined the benefits of this controller during the platoon formation process.

Commented [SW40]: Double check throughout document the proper casing for "algorithm".

Commented [SW41]: Is this different than "StPF" algorithm?

Commented [MN42R41]: Yes. In StPF, we will control only one truck. SiFPA is intended to be used for passenger cars, where we can manipulate them as a group (like flocking) to form platoons.

Commented [SW43]: This material is more appropriate in the Conclusions section.

7.0 REFERENCES

Ahmed, K.I., 1999. *Modeling drivers' acceleration and lane changing behavior* (Doctoral dissertation, Massachusetts Institute of Technology).

Bang, S. and Ahn, S., 2017. Platooning strategy for connected and autonomous vehicles: transition from light traffic. *Transportation Research Record*, *2623*(1), pp. 73-81.

Barth, M., Younglove, T. and Scora, G., 2005. Development of a heavy-duty diesel modal emissions and fuel consumption model.

Belzile, M., Patten, J., Eng, P., McAuliffe, B., Mayda, W. and Tanguay, B., 2012. Technical Report Review of Aerodynamic Drag Reduction Devices for Heavy Trucks and Buses. *Project*, *54*, p.A3578.

Cohen, S.L., 2002. Application of car-following systems in microscopic time-scan simulation models. *Transportation research record*, *1802*(1), pp. 239-247.

Contet, J.M., Gechter, F., Gruer, P. and Koukam, A., 2007, October. Application of reactive multiagent system to linear vehicle platoon. In *19th IEEE International Conference on Tools with Artificial Intelligence (ICTAI 2007)* (Vol. 2, pp. 67-70). IEEE.

Deng, Z., Fan, J., Shi, Y. and Shen, W., 2022. A coevolutionary algorithm for cooperative platoon formation of connected and automated vehicles. *IEEE Transactions on Vehicular Technology*, *71*(12), pp.12461-12474.

El Ganaoui-Mourlan, O., Camp, S., Hannagan, T., Arora, V., De Neuville, M. and Kousournas, V.A., 2021. Path planning for autonomous platoon formation. *Sustainability*, *13*(9), p. 4668.

Feng, Shuo, Yi Zhang, Shengbo Eben Li, Zhong Cao, Henry X. Liu, and Li Li. "String stability for vehicular platoon control: Definitions and analysis methods." *Annual Reviews in Control* 47 (2019): 81-97.

Gao, F., Li, S.E., Zheng, Y. and Kum, D., 2016. Robust control of heterogeneous vehicular platoon with uncertain dynamics and communication delay. *IET Intelligent Transport Systems*, *10*(7), pp. 503-513.

Gong, S. and Du, L., 2018. Cooperative platoon control for a mixed traffic flow including human drive vehicles and connected and autonomous vehicles. *Transportation research part B: methodological*, *116*, pp. 25-61.

Guo, G., Li, P., and Hao, L.Y., 2020. Adaptive fault-tolerant control of platoons with guaranteed traffic flow stability. *IEEE Transactions on Vehicular Technology*, *69*(7), pp. 6916-6927.

Commented [SW44]: 46-68?

Commented [MN45R44]: It is 4668 - starts from page 4668 of the journal. (p, not pp)

Commented [46R44]: Typically, you put the range of pages, not just the starting page.

Commented [MN47R44]: I rechecked the citations from the journals. They seem to refer to the article number and not the page numbers.

"Note that from the first issue of 2016, this journal uses article numbers instead of page numbers. See further details here."

Commented [SW48]: Should there be a comma in between the "Li"'s?

Li, D. and Guo, G., 2020. Prescribed performance concurrent control of connected vehicles with nonlinear third-order dynamics. *IEEE Transactions on Vehicular Technology*, *69*(12), pp. 14793-14802.

Li, Q., Chen, Z., & Li, X. (2022). A review of connected and automated vehicle platoon merging and splitting operations. *IEEE Transactions on Intelligent Transportation Systems*, *23*(12), 22790-22806.

Li, S.E., Zheng, Y., Li, K., Wu, Y., Hedrick, J.K., Gao, F. and Zhang, H., 2017. Dynamical modeling and distributed control of connected and automated vehicles: Challenges and opportunities. *IEEE Intelligent Transportation Systems Magazine*, *9*(3), pp.46-58.

Li, Y., Zhong, Z., Song, Y., Sun, Q., Sun, H., Hu, S. and Wang, Y., 2020. Longitudinal platoon control of connected vehicles: Analysis and verification. *IEEE Transactions on Intelligent Transportation Systems*, *23*(5), pp.4225-4235.

Li, Z., Khasawneh, F., Yin, X., Li, A. and Song, Z., 2019. A new microscopic traffic model using a spring-mass-damper-clutch system. *IEEE Transactions on Intelligent Transportation Systems*, *21*(8), pp.3322-3331.

Liang, K.Y., Deng, Q., Mårtensson, J., Ma, X., and Johansson, K.H., 2015, June. The influence of traffic on heavy-duty vehicle platoon formation. In *2015 IEEE Intelligent Vehicles Symposium (IV)* (pp. 150-155). IEEE.

Maiti, S., Winter, S., Kulik, L. and Sarkar, S., 2019. The impact of flexible platoon formation operations. *IEEE Transactions on Intelligent Vehicles*, *5*(2), pp. 229-239.

Milanés, V. and Shladover, S.E., 2014. Modeling cooperative and autonomous adaptive cruise control dynamic responses using experimental data. *Transportation Research Part C: Emerging Technologies*, *48*, pp.285-300.

mobility.tamu.edu. (n.d.). *Urban Mobility Report — Urban Mobility Information*. [online] Available at: https://mobility.tamu.edu/umr/.

Munigety, C.R., 2018. A spring-mass-damper system dynamics-based driver-vehicle integrated model for representing heterogeneous traffic. *International Journal of Modern Physics B*, *32*(11), p. 1850135.

Qiu, J. and Du, L., 2023. cooperative trajectory control for synchronizing the movement of two connected and autonomous vehicles separated in a mixed traffic flow. *Transportation Research Part B: Methodological*, *174*, p. 102769.

Shladover, Steven E., Christopher Nowakowski, Xiao-Yun Lu, and Robert Ferlis. "Cooperative adaptive cruise control: Definitions and operating concepts." *Transportation Research Record* 2489, no. 1 (2015): 145-152.

Commented [SW49]: Check this.

Commented [SW50]: Check this.

Van Arem, B., Van Driel, C.J. and Visser, R., 2006. The impact of cooperative adaptive cruise control on traffic-flow characteristics. *IEEE Transactions on intelligent transportation systems*, *7*(4), pp. 429-436.

Wang, Z., Mi, Q., Xiang, J., Zhang, Z., & Tang, J. (2024). An evaluation of lane management strategy for CAV priority in mixed traffic. *IET Intelligent Transport Systems*, *18*(3), 467-479.

Woo, S. and Skabardonis, A., 2021. Flow-aware platoon formation of Connected Automated Vehicles in a mixed traffic with human-driven vehicles. *Transportation research part C: emerging technologies*, *133*, p.103442.

Xie, S., Hu, J., Ding, Z. and Arvin, F., 2022. Cooperative adaptive cruise control for connected autonomous vehicles using spring damping energy model. *IEEE Transactions on Vehicular Technology*, *72*(3), pp. 2974-2987.

Zabat, M., Stabile, N., Frascaroli, S. and Browand, F., 1995. The aerodynamic performance of platoons. *University of California, Tech. Rep*.

Zhang, H., Du, L. and Shen, J., 2022. Hybrid MPC system for platoon based cooperative lane change control using machine learning aided distributed optimization. *Transportation Research Part B: Methodological*, *159*, pp. 104-142.

Fast facts on transportation greenhouse gas emissions | US EPA (2023). https://www.epa.gov/greenvehicles/fast-facts-transportation-greenhouse-gas-emissions.

Florida Traffic Online. (no date). https://tdaappsprod.dot.state.fl.us/fto.

California Partners for advanced transportation technology (no date). https://path.berkeley.edu/.

Mobility Division (2022) *Urban Mobility Report - Mobility Division*. https://mobility.tamu.edu/umr.

US Census Bureau (2024a) *Annual Retail Trade Survey Supplemental E-commerce Tables: 2022*. https://www.census.gov/data/tables/2022/econ/arts/supplemental-ecommerce.html.

US Census Bureau (2024a) *Annual Retail Trade Survey: 2022*. https://www.census.gov/data/tables/2022/econ/arts/annual-report.html.

Washburn, S.S. *SwashSim Documentation*. 2024. https://github.com/swash17/SwashSim.

Commented [SW51]: Check this.